Sule Lamido University Journal of Science & Technology Vol. 7 No. 1 [June, 2023], pp. 97-115
https://doi.org/10.56471/slujst.v7i.380

Online ISSN: 2736-0903
Print ISSN: 2736-089X
www.slujst.edu.ng

Evaluating the Performance of Machine Learning Algorithms and Maximum Likelihood Classifier for Land-Use and Land-Cover Change Detection in Yola, Nigeria

Muhammad Isma'il[1*], Sule Muhammad Zubairu[2], Auwal Aliyu[3], Muhammad Hadi Ahmed[4], Sadiq Ibrahim[5], Abubakar Magaji[6] and Idris Moisule Hassan[7]

[1,2]Department of Geography and Environmental Management, Ahmadu Bello University, Zaria.

[3,4,5,6,7]National Space Research and Development Agency, Zonal Advanced Space Technology Application Laboratory, Kano

migeogjameel@gmail.com[1*], sulemuhd@gmail.com[2], auwalaliyu508@gmail.com[3], telnettoahmad@gmail.com[4], sadeeqibraheem992@gmail.com[5], abdullahiabubakar117@gmail.com[6], chemicalreader094@gmail.com[7]

[*]Corresponding Author

Abstract

The availability of high-end consumer computing power and free satellite data has caused data science and remote sensing groups to begin aligning in recent years. Openly accessible data from the Landsat series of the United States Geological Survey (USGS) have been used in a number of remote sensing applications. Nevertheless, there is a lack of studies that utilize these data to evaluate the performance of machine learning algorithms and maximum likelihood for LULC classification in the complex Yola-North Landscape. In this study, we compared the classification performance of support vector machines (SVM), Artificial Neural Network (ANN) machine learning algorithms and maximum likelihood parametric algorithm. The study area chosen is a complex mixed-use landscape with four major land use and land cover (LULC) classes built-up, vegetation, water and bare soil. Multi-temporal scenes from Land sat 7 ETM+ and Land sat 8 OLI images covering the period of 2002, 2012 and 2022 were used for the classification. Accuracy was assessed using Overall Accuracy and Kappa Coefficient derived from an error matrix. The Land Change Modeler (LCM) was used to detect changes in the LULC. The results show that the highest overall accuracy was achieved by support vector machines (95.5%, 87.7% and 90%) for year 2022, 2012 and 2002 respectively, closely followed by Artificial Neural Network (89.5%, 87.5% and 85%) for 2022, 2012 and 2002 respectively, and finally, Maximum Likelihood (between 84.5% and 70%). The findings also show that, the built-up areas have increased significantly, this increase coincided with a decrease in vegetation area, bare surface and water, and without proper planning it could cause a severe consequence for the environment, society, and overall sustainability. By prioritizing sustainable development, integrating smart growth principles, and fostering collaboration among stakeholders, it is possible to mitigate these negative effects and create more resilient, livable, and equitable urban environments.

Keywords: *Classification, Land use Land cover (LULC) Change, Machine learning, Support vector Machine, Artificial Neural Network, Maximum likelihood, classifier.*

1. Introduction

Land is one of the most significant natural resources because it is the foundation of all life and many developmental activities. Land cover, changes as a result of poor land resource management (Ayele et al., 2018). Changes in land use and land cover (LULC) have been highlighted as one of the most major causes of ecosystem changes that are causing social and environmental problems around the world, such as disasters and climate change (Nedd et al., 2021). Yola North Local Government Area (LGA) is the largest urban area in Adamawa State and it is expanding due to inflow of people seeking to benefit from available economic activity. Construction of infrastructure and housing developments, which result in the loss of agricultural land, are the most important drivers

Online ISSN: 2736-0903
Print ISSN: 2736-089X
www.slujst.edu.ng

of land cover change in this region. Understanding the dynamics of this changing environment necessitates continuous monitoring of Land Use and Land Cover (Abera et al., 2021). Satellite remote sensing data have shown to be highly beneficial in mapping land use/ land cover patterns due to their repetitive nature and the availability of reliable geo-referencing processes (Adhikary et al., 2019). Geographic Information System (GIS) technology, which offers a scientific method to analyze pattern, rate, and trend of environmental change, makes it possible to quantify such changes (Ayele et al., 2018). Delalay et al. (2019) Opines that LULC classification is important for Land use change analysis and it refers to the task of identifying category of every pixel in an image. Selection of the best classifier is a fundamental problem to solve in order to improve LULC classification because of complexity of ground covers (Yan et al., 2019). The recent past has seen a sharp increase in the ease of access to satellite imagery data and cloud computing platforms, as well as substantial progress in classification techniques. A series of conventional classification methods have been well developed and long used for remote sensing applications, which are Parallelepiped, Minimum Distance, and Maximum Likelihood (ML) models. Many other advanced Machine learning classification techniques have also been introduced in the field of Remote Sensing, including Artificial Neural Networks, Decision Trees, Random Forest and Support Vector Machine. For instance, Abdi (2020), evaluated the performance of Support Vector Machine (SVM), Random forest (RF), Extreme gradient boost (Xgboost) and Deep Learning (DL) for Land use land cover classification on sentinel-2 image in a boreal landscape in south-central Sweden. On the other hand, Leeuwen et al. (2020) compared Random Forest, Support Vector Machine and an Artificial Neural Network for LULC classification in a south of Hungray, while Traore et al. (2019) Used Support Vector Machine on Multi-Temporal Landsat Images to Assess the Changes in Agricultural Irrigated Areas in the Mogtedo Region, Burkina Faso, between 1987 and 2015.

Machine learning is a branch of Artificial Intelligence (AI) and Computer Science, which focuses on the use of data and algorithms to imitate the way that humans learn (International Business Machine [IBM], 2020). This implies that machines are capable of doing a task in the real world or recognizing a visual scene. Supervised Machine Learning, also known as, Supervised Learning is one form of Machine Learning that use labeled datasets to train algorithms that to classify data or predict outcomes accurately with statistical methods (IBM, 2020). Image classification has made tremendous progress as a result of the advent of machine Learning classification methods, particularly Support Vector Machine (SVM) and Artificial Neural Network (ANN), as well as the availability of high-resolution remote sensing data (Nogueira et al., 2017). Support Vector Machine is a supervised machine learning classification method that provides for precise classifications from a small number of training sites (Birzhandi et al., 2022). Classification errors are minimized using the SVM approach by constructing a hyperplane between each class that maximizes the distance between the support vectors of each class (Rendy, 2021). A neural network is a type of supervised learning classifier that models human neural connections. It is a supervised learning model that leverages brain functioning as a foundation to construct algorithms for classification and prediction. ANN, unlike other prediction algorithms, does not place constraints on input variables and may generalize and forecast on unseen data (Shih et al., 2019).

The Maximum Likelihood classifier is one of the most prevalent methods of classification in remote sensing, in which a pixel with the highest likelihood is categorized into the appropriate class. It is a statistical decision criterion used to aid in the classification of overlapping signatures. Pixels are given to the class with the highest probability (Soni, 2011). Maximum Likelihood (ML), a parametric method, has been widely tested with per-pixel image classification tasks on medium and low-resolution satellite images (Faisal et al., 2021; Muhammad et al., 2018). However, the challenges associated with LULC classification based on time series remain; this technique is primarily hampered by insufficient sampling used to train the supervised algorithms (Petitjean et al., 2012), along with the brightness of an image brought on by variations in the effects of atmosphere and illumination, which led to a number of spectral and spatial limitation that have an impact on its accuracy (Yu et al., 2020). Machine learning approaches such as ANN and SVM, which have shown significant improvement in classification accuracy, have challenged such frequently used classification techniques (Hamad, 2020; Valero and Alzate, 2019). This study present and compare the performance of different classification methods for LULC classification and detection of LULC change in Yola North L.G.A. through the remote sensing data processing which has implication on quality, and integrity of outputs, because, good result depends on the model set-up, sample size and

Sule Lamido University Journal of Science & Technology Vol. 7 No. 1 [June, 2023], pp. 97-115
https://doi.org/10.56471/slujst.v7i.380
Online ISSN: 2736-0903
Print ISSN: 2736-089X
www.slujst.edu.ng

characteristics of the study area (Talukdar et al., 2020). Hence the objectives of this study are to: 1- generate LULC maps using Machine learning and Maximum likelihood classifiers, 2-compare LULC maps using Machine learning and Maximum likelihood classifiers, 3-Detect LULC change between 2002 and 2022.

2. Study Area

Yola-North LGA is one of the largest cities in Adamawa state, Nigeria, situated at a height of 215 meters Above Mean Sea Level and located between Latitudes 9° 12' 0." and 9° 21' 0" North of the Equator and Longitudes 12° 19' 12" and 12° 30' 0" East of the Greenwich Meridian. The area is located at the bank of River Benue and is bounded by Giere in the North and East, and in South and West by Yola-South local government area. Yola-North Local Government is composed of eleven Wards namely; Yelwa, Nasarawo, Jambutu, Luggere, Alkalawa, Doubeli, Limawa, Rumde, Karewa, Ajiya and Gwadabawa. It has an estimated area of approximately112.74Km².

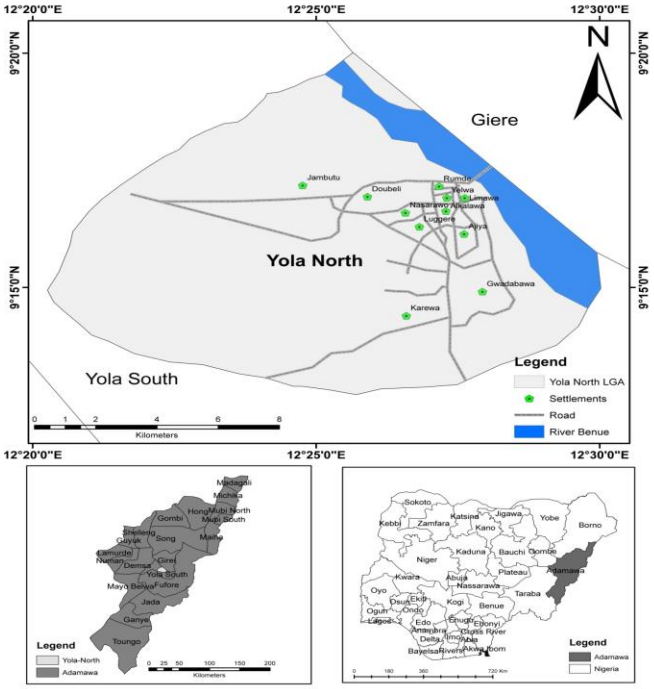

Figure 1. The Study Area: Yola-North LGA (Source: Adapted and modified from the Administrative Map of Nigeria)

Yola North Local Government area experiences a tropical sub humid climate, the wet and dry seasons. Over the course of the year, the temperature typically varies from *17° Celsius (C) to 39° Celsius (C)* and is rarely below *14°Celsius (C)* or above *42° Celsius (C) (Weather spark, 2021)*. The population of the area is approximately 316,459 based on exponential growth model with an annual growth rate of 2.92 percent ("Jimeta Population", 2015). The city is clearly stratified in terms of population densities such as low, medium and high-density areas.

3. Methodology

3.1 Types and Sources of data

Satellite images, Ground truth points, road network, Digital Elevation Model (DEM) as well as Administrative boundary were used for studying the LULC change in the study area. The classification was performed on a multi-temporal set of optical Landsat images. They have a ground sampling distance of 30 meters and cover the optical electro-magnetic spectrum in several bands obtained from United State Geological Survey (USGS). The satellite data for this study comprised images of the study area for three time periods 2002, 2012 and 2022. The 2002 and 2012 images were scene of a Landsat-7 Enhanced Thematic Mapper Plus with a path and row

SLUJST
Sule Lamido University Journal of Science & Technology Vol. 7 No. 1 [June, 2023], pp. 97-115
https://doi.org/10.56471/slujst.v7i.380
Online ISSN: 2736-0903
Print ISSN: 2736-089X
www.slujst.edu.ng

of 185 and 54 respectively, taken on February 17, 2002 and February 13, 2012, while the 2022 image was a scene of landsat 8 Operational Land imager with a path/row of 185/54, taken in February 16, 2022. Both images were acquired from the archive of United State Geological Survey (USGS) Earth Resources Data website (http://www.earth explorer.usgs.gov). The images were of high quality and free from cloud cover. The only problem had to do with scan-line-off error of Landsat-7 ETM+ of 2012. A samples size of 50 ground truth points for each land use Land cover class category (Anad, 2017) making a total of 200 sample size were obtained from field based on stratified random sampling (Anad, 2017) while the administrative boundary of the study area was extracted from the administrative map of Nigeria. On the other hand, affective variable for Land Change Modeler (LCM) such as Road network and Digital Elevation Model (DEM) were obtained from DIVA GIS and USGS respectively. The types and Sources of data are presented in Table 1.

Table 1. Types and Sources of data

Types of Data	Source	Purpose
Landsat-7 ETM+	USGS	LULC classification (2002/2012)
Landsat-8 OLI	USGS	LULC classification (2022)
Ground truth points	Study area	Accuracy assessment
Administrative boundary	Admin. Map of Nigeria	Subseting
Road network	Diva GIS	Change analysis
DEM	USGS	Change analysis

3.2 Pre-processing

The methodology adopted for this study took into consideration various image pre-processing operations, including elimination of Scan line errors and Radiometric and atmospheric correction. It began with the elimination of scan line errors which correct the scan line that traces a zigzag pattern along the satellite imaged area (USGS, 2022). A fix land sat 7 scan line error tool was used in order to reduce the influence of scan line errors in the land sat 7 (2012) images. Afterwards a basic atmospheric correction was performed on the images; this includes Digital Number (DN) to top-of-atmosphere reflectance conversion. Furthermore, the three images of each acquisition date were layer stacked which are useful in visualizing and identification of urban, vegetation, water and bare surface and discriminate features that look similar (as in Ettehadi, 2019), and finally the layer stacked images were subset, in order to save disk space and processing time for better handling of the images. The atmospheric and radiometric correction was carried out using the following formula. Radiometric and Atmospheric correction formula:

$$P\lambda = \frac{M\rho * DN + A\rho}{Sin(\theta SE)} \quad (1)$$

Where: Pλ = Top of atmosphere Planetary Reflectance (Corrected image)
DN = Digital Number (Band Specific Satellite image)
Mρ= Band Specific Reflectance_ Multi_Band Value
Aρ = Band Specific Reflectance_Add_Band Value
Adapted and Modified from Das (2021)

3.3 Selection of training sites

In this study, supervised classification methodologies were used to classify the LULC categories into the four classes (Built-up, Vegetation, Water and Bare surface) that were identified based on the visual interpretation of the satellite imagery and verified from reconnaissance survey. Combining training sites with prior knowledge and familiarity with the study area is necessary to complete the supervised classification (Jensen, 2005). Supervised classification necessitates the use of training sites to define the spectral reflectance pattern or signature of each LULC category. Training data have generally showed to have a great impact on the accuracy of the classification as it determines which class each pixel inherits in the overall image. The training sites were chosen based on the four broad LULC classes in the study area which include Built-up, Vegetation, Water and Bare surface. Sand and bare lands were merged into one LULC class (Bare surface) because it was difficult to differentiate these bodies in view of their relatively small portion in the study area. For SVM and ANN classification, training site are selected

Sule Lamido University Journal of Science & Technology Vol. 7 No. 1 [June, 2023], pp. 97-115
https://doi.org/10.56471/slujst.v7i.380
Online ISSN: 2736-0903
Print ISSN: 2736-089X
www.slujst.edu.ng

using ENVI 5.3, the general process began by defining polygons around representative portions of each LULC category in each Landsat image using Region of Interest (ROI) tools and functions for SVM and ANN classification, which were used to train and apply the classifiers. Similar but different software interface and specific steps following workflow of data preparation, training site selection, digitization, attribute assignment, training sample collection, classifier configuration, classification training and classification execution were used for maximum likelihood in Arcmap10.8 using Image Classification tool. The respective Land use and Land cover classes are described in Table 2.

Table 2. Description of LULC classes in Yola North L.G.A

LULC	Description
Built-up	Housing, Asphalt roads, markets, institution, public and private offices
Vegetation	Agricultural lands, trees and grasses.
Water	River, Ponds and streams
Bare surface	Undeveloped land, land without vegetation cover and sand.

3.4 Accuracy Assessment

Accuracy assessment is critical in any classification project since it compares the classified image to ground truth data from the study area that is regarded accurate to establish the quality of information derived from remotely sensed data (Anad, 2017). A minimum of 50 samples size of ground truth points for each land use Land cover class category collected based on stratified random sampling (Anad, 2017) were used. Confusion matrix technique (as in Congalton and Green, 2019) was used to statistically analyze ground truth points data and classification results, after which the results were used to compare the three classification algorithms (SVM, ANN as well as ML), and select the result with highest accuracy. These standards error matrices were computed based on the same data references for each image to calculate the components of overall accuracy (see Equation 2), producer and user accuracy (see Equation 3 and Equation 4 respectively), as well as kappa coefficient (see Equation 5) as stated by many studies such as Aljenaid et al., 2021; Sophia and Julius, 2017; Adeyemi and Oyeleye, 2021.

Overall Accuracy (OA):

$$\mathrm{OA} = \frac{\text{Total No of accurately classified pixel}}{\text{Total No of Reference pixel}} \times 100 \qquad (2)$$

Producer Accuracy (PA):

$$\boldsymbol{PA} = \frac{\text{Samples correctly identifiied in the column}}{\text{Column total}} \times 100 \qquad (3)$$

User Accuarcy (UA):

$$\boldsymbol{UA} = \frac{\text{Samples correctly identifiied in the Row}}{\text{Row total}} \times 100 \qquad (4)$$

Kappa coefficient (T):

$$\mathrm{T} = \frac{(TS*TCS) - \Sigma\,(\mathrm{CT}*\mathrm{RT})}{TS^2 - \Sigma\,(\mathrm{CT}-\mathrm{RT})} \qquad (5)$$

Where: T = Kappa Coefficient, TS = Total sample, TCS = Total correctly classified sample, CT = Column Total, RT = Row Total

Overall accuracy above 85% (Anderson *et al.*, 1976) and Kappa value above 0.75 (Fleiss *et al.*, 2003) were the threshold used to determine the classifier that met the minimum level of accuracy for the classified maps.

3.5 Change detection

Change detection aims to compare the spatial representation of two points in time while controlling all variations due to differences in the variables of interest (Green *et al.*, 1994).To detect the changes in LULC between

Sule Lamido University Journal of Science & Technology Vol. 7 No. 1 [June, 2023], pp. 97-115
https://doi.org/10.56471/slujst.v7i.380
Online ISSN: 2736-0903
Print ISSN: 2736-089X
www.slujst.edu.ng

2002, 2012 and 2022, Land Change Modeler (LCM) and Descriptive statistics were used. Prior land use belongs to previous years (2002 and 2012) and Current land use (2022) as well as affective variables on land use changes (Such as Road and Digital Elevation Model) were fed into the LCM model embedded in the Idrissi Selva software to evaluate the patterns and trend of LULC changes, as well as the matrix of change between LULC classes. Incorporating Road and elevation data enables a more comprehensive understanding of the spatial patterns and drivers of land cover change, contributing to more accurate and informed decision-making processes related to land management, conservation, and environmental planning. The LCM model integrated the mentioned layers to predict change detection. The areas covered by each land use type for the three periods were compared. Then the directions of the changes (positive or negative) in each land use type 2002, 2012 and 2022 were determined. The methodology adopted in this work is shown in the Figure 2 below:

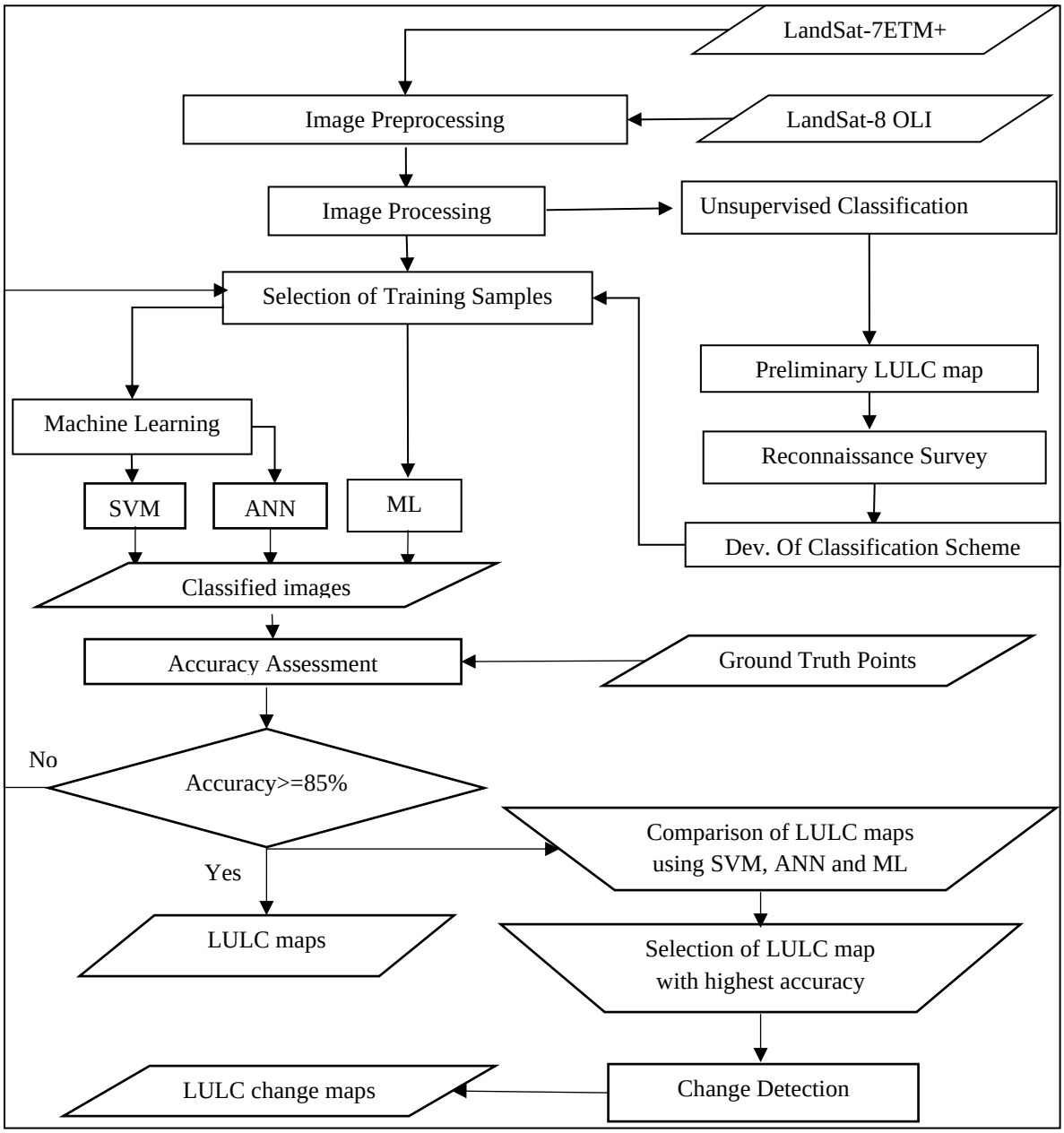

Figure 2: Flowchart of the Methodology

SLUJST
Sule Lamido University Journal of Science & Technology Vol. 7 No. 1 [June, 2023], pp. 97-115
https://doi.org/10.56471/slujst.v7i.380
Online ISSN: 2736-0903
Print ISSN: 2736-089X
www.slujst.edu.ng

4. Result and Discussion

4.1 Classified images

4.1.1 LULC Maps using Support Vector Machine

Figure 3 presents the multi-temporal LULC with four major classes; Vegetation, Bare soil, built-up area and water bodies of 2002, 2012, and 2022 generated by SVM. Table 3 revealed that in 2002, bare soil occupied 74,462 km² (66.02%) mainly around the western part of the study area. This was followed by vegetation with 18.486 km² (16.40%), which was scattered around the north, south, and eastern parts of the area. Built-up covered 16.481 km² (14.62%) of the area, located mainly around the central part of the area. water bodies were least with 3.347 km² (2.97%) located mainly at north eastern part of the area. In 2012, built-up increased to 44.257 km² covering 39.26% of the area, with concentration in most part of the area except in an area dominated by water bodies that increased to 3.921 km² (3.34%). bare soil decreased to 47.981 km² (42.56%), and vegetation also reduced to, 16.581 km² (14.71%) with concentration within the region where people farm and very few scattered ones in other areas. In 2022, Built-up occupied 58.556 km² (51.94%) with an increase of 12.68% in 20 years (from the previous period). Water bodies, however declined by 1.05%, to 2.683 km² (2.38%), within the same period. bare surface covered 36.701 km² (32.55%) representing a decline of 11.28% from previous period. Similarly, vegetation contrasted by 1.58% to 14.800 km² (13.13%).

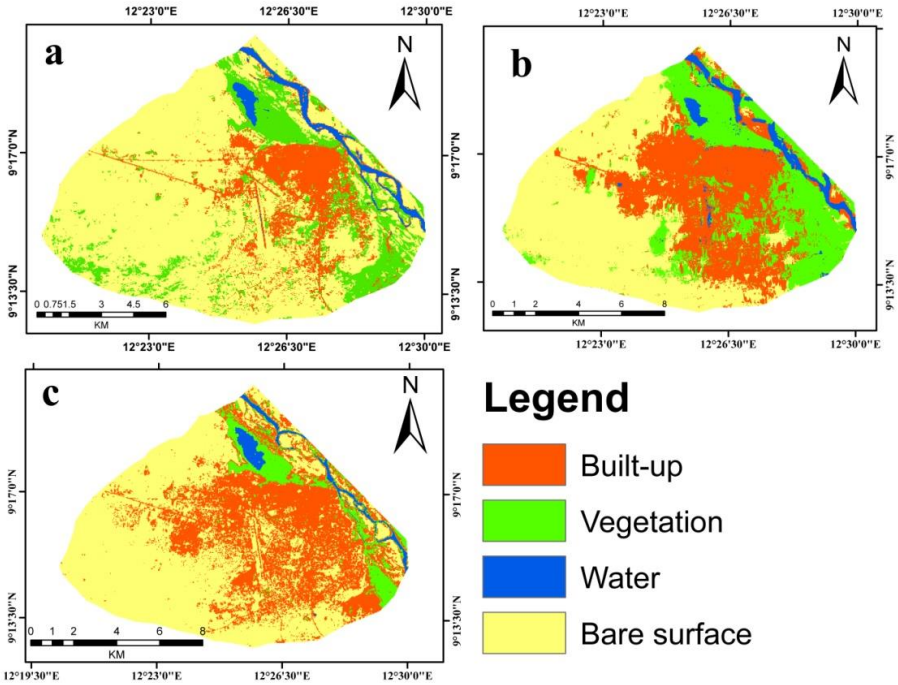

Figure 3. Final classified Land use and land cover using SVM for (a) 2002, (b) 2012 and (c) 2022

Table 3. Spatial distribution of LULC status using Support Vector Machine

	2002		2012		2022	
LULC	**Area (Km²)**	**%**	**Area (Km²)**	**%**	**Area (Km²)**	**%**
Built-up	16.481	14.62	44.257	39.26	58.556	51.94
Vegetation	18.486	16.40	16.581	14.71	14.800	13.13
Water	3.347	2.97	3.921	3.48	2.683	2.38
Bare surface	74.426	66.02	47.981	42.56	36.701	32.55
Total	**112.74**	**100**	**112.74**	**100**	**112.74**	**100**

SLUJST
Sule Lamido University Journal of Science & Technology Vol. 7 No. 1 [June, 2023], pp. 97-115
https://doi.org/10.56471/slujst.v7i.380
Online ISSN: 2736-0903
Print ISSN: 2736-089X
www.slujst.edu.ng

According to the result, from the previous decades, bare soil and vegetation have declined since 2002 while, Built-up area have increased which shows that increase in building infrastructure, probably due to population expansion and its demand for infrastructural development cause a considerable change in LULC. The landsat 8 (OLI TIRS) image used for LULC classification in 2022 has a better spectral quality which allows identification of built-up areas, vegetation, bare surface and water body. SVM showed robustness in classification of land sat 7 ETM (2012) even though the image had poor quality. SVM had a high processing speed, however, it poorly generalizes the images. SVM produced visually appealing result that fairly depicted the region, with coherent classes and little speckling. This implies that all the LULC features are properly delineated by SVM. This is in line with the result of kadavi and lee (2018) who reported that, LULC features were fairly delineated by SVM in a land cover classification of volcanic island in Aleytian Arc, USA and also Abdi (2020) noted that, SVM had properly delineated boreal landscape and maintain a high recognition rate in the Land use land cover classification in south central Sweden. Consequently, it can be concluded that the SVM was computationally efficient and had a high recognition rate.

4.1.2 LULC maps using Artificial Neural Network

Similarly, the spatial analysis of the LULC of 2002 generated by ANN shows that bare surface covered the largest portion of total area as shown in Figure 4, but representing 93.07km² (82.55%), followed by vegetation 9.61km² (8.52%), while built-up area occupied 7.30km² (6.48%) of the total land area. water is the least covering an area of 2.75 km² (2.44%) in the output (Table 4). Between 2002 and 2012, bare soil sharply contrasted by 25.76% to 64.02km² (56.79%) of the land area. built-up gained 27.01% to occupy 38.68km² (34.31%) within the period. Water bodies were down by 0.12% with 2.96km² (2.63%). There was also a decreased of 2.23% in vegetation cover at 7.09km² (6.29%) within that period (Table 4).

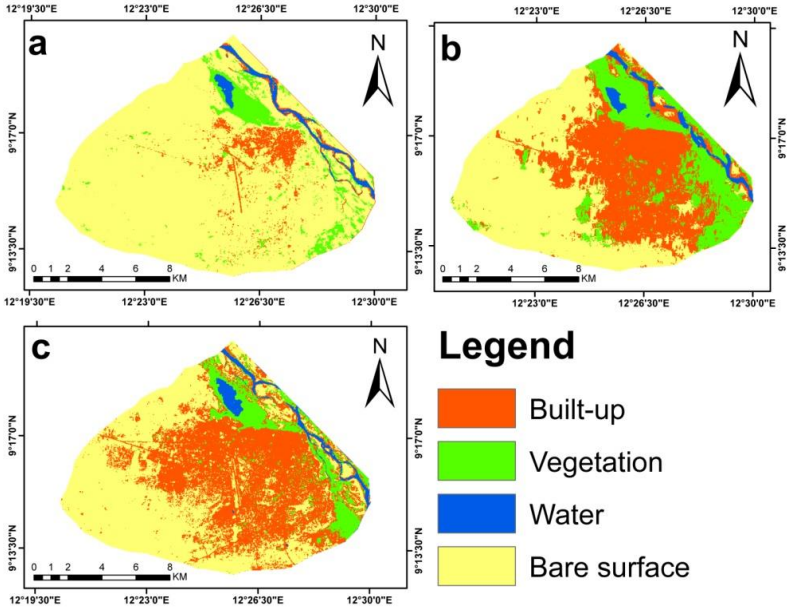

Figure 4. Final classified Land use and land cover using ANN for (a) 2002, (b) 2012 and (c) 2022

Table 4. Spatial Distribution of LULC status in Yola North using Artificial Neural Network

	2002		2012		2022	
Classes	Area (Km^2)	%	Area (Km^2)	%	Area(Km^2)	%
Built-up	7.30	6.48	38.68	34.31	44.50	39.48
Vegetation	9.61	8.53	7.09	6.29	5.88	5.21
Water	2.75	2.44	2.96	2.62	3.21	2.85
Bare surface	93.07	82.56	64.02	56.79	59.15	52.46
Total	**112.74**	**100**	**112.74**	**100**	**112.74**	**100**

SLUJST
Sule Lamido University Journal of Science & Technology Vol. 7 No. 1 [June, 2023], pp. 97-115
https://doi.org/10.56471/slujst.v7i.380
Online ISSN: 2736-0903
Print ISSN: 2736-089X
www.slujst.edu.ng

In 2002, as estimated by SVM, bare surface is the most dominant land-use class in the region classified by ANN classifier. It covers over half of the total land surface. Vegetation and Built-up are at the second and third positions respectively in terms of areal share, while the Water has the least share in the total land surface area. The classification result established by ANN also indicates significant increase in the Built-up area in Yola North between 2002 and 2022. This agrees with classification result generated by SVM algorithm which indicated forward trend in Built-up over the study period. ANN was able to generalize the image, but poorly classified the land 7 ETM (2012) probably due to its poor spectral quality. Most pixels which belong to classes were correctly classified. This is in accordance with Hamad (2020) who noted that most pixel were correctly classified by ANN, for Land cover classification using sentinel 2A in city of Soran, Kudistan Region, Iran**.** The result also revealed problems of mis-classification of LULC features for all the three years. Some part of built-up, water and Vegetation of the subset are misclassified as bare surface. This is an indication that ANN over estimated bare surface and under estimated Built-up, water and Vegetation for all the three years. This result agrees with the result of Moumni and Lahrouni (2021) who reported problems of mis-classification by Artificial Neural Network, in a crop type classification using Sentinel 1 and 2 data in semiarid area of central Morocco.

4.1.3 LULC maps using Maximum Likelihood Classifier

The study produced four thematic land cover maps from the various pre-processing operations conducted alongside the supervised classification using the maximum-likelihood algorithm of the satellite images in 2002, 2012, and 20202 as shown in Figure 5. These maps provided the land cover classification of the study area comprising four distinct classes: built-up/urban areas, vegetation, water bodies, and bare soil. The red color on the map signifies the built-up area; the green color shows the vegetation cover, the blue color signifies water bodies, while the yellow color signifies the bare soil. The spatial distribution of each land cover class was extracted from the individual classified map, and the result was quantified in Table 5. The vegetation covered an area of 10.76km² (9.55%) in 2002 and gradually decreased to 5.59km² (4.96%) in 2022. For other land cover classes, the results have shown that the built-up area had rapidly increased from 8.07km² (7.16%) in 2002 to approximately 44.47km² (39.45%) in 2022. The area of the water bodies increased slightly from 2.21km² (1.96%) in 2002 to about 2.39km² (2.12%) in 2022. During the same period, Yola' bare surface decreased slightly from 91.69km² (81.33%) in 2002 to 60.29km² (53.47%) in 2022.

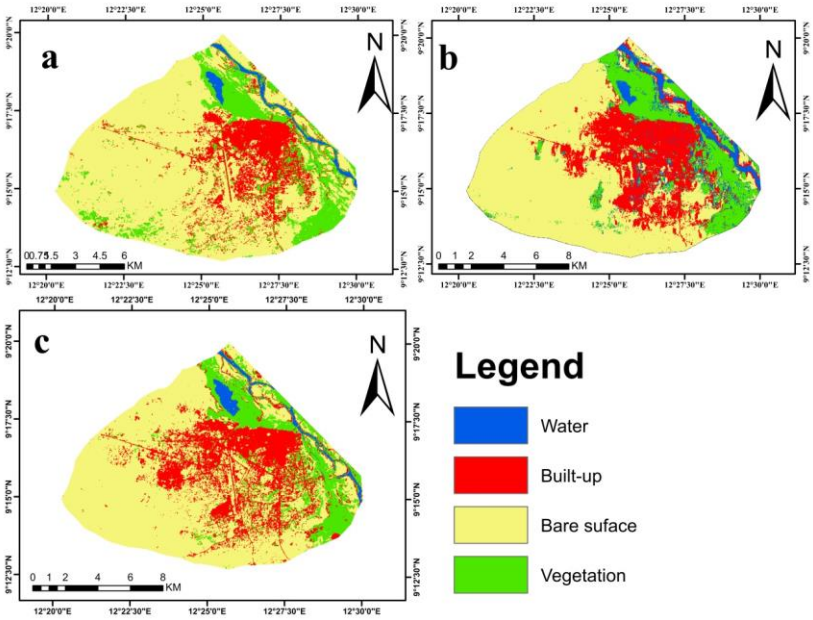

Figure 5. Maximum Likelihood final classified Land use and Land cover maps for (a) 2002, (b) 2012 and (c) 2022.

SLUJST
Sule Lamido University Journal of Science & Technology Vol. 7 No. 1 [June, 2023], pp. 97-115
https://doi.org/10.56471/slujst.v7i.380
Online ISSN: 2736-0903
Print ISSN: 2736-089X
www.slujst.edu.ng

Table 5. Spatial Distribution of LULC status in Yola North using Maximum Likelihood

	2002		2012		2022	
Classes	**Area (Km^2)**	**%**	**Area (Km^2)**	**%**	**Area (Km^2)**	**%**
Built-up	8.07	7.16	33.94	30.11	44.47	39.45
Vegetation	10.76	9.55	8.59	7.62	5.59	4.96
Water	2.21	1.96	7.47	6.62	2.39	2.12
Bare surface	91.69	81.33	62.74	55.65	60.29	53.47
Total	**112.74**	**100**	**112.74**	**100**	**112.74**	**100**

The classification result by ML also established significant changes in the different land cover classes in Yola North between 2002 and 2022. As found by SVM and ANN, A remarkable increase in built-up areas was observed and a considerable decrease in areas covered by vegetation and bare soil, as shown in figure 5. This is in harmony with (Muhammad *et al.*, 2018) who reported that a built-up area in Yola North Local Government area is increasing. The dominance of the built-up confirms that the city is experiencing urban growth probably due the population expansions that led to infrastructural development. The result of the classification also revealed that Maximum likelihood classifier achieved a good differentiation of coverage in non-sampled areas of the images. This result agrees with the result obtained by Valero and Alzate (2019) who report that a good differentiation of coverage in non-sampled areas was achieved by Maximum likelihood, in a comparison of SVM, ML and RF for Land cover classification in San Pelayo, Colombia. Nonetheless, as in the output of ANN, the classification resulted in misclassification of Built up, vegetation as bare surface and water as Vegetation for all the three years. This implies that there are overestimations of bare surface and under estimation of built-up which is probably due to the nature of the classifier which require sufficient training sites to produce accurate LULC map. The preceding claims are validated in a crop type mapping by Moumni and Lahrouni (2021) in semiarid area of central Morocco, who reported that there were over estimation of LULC features by maximum likelihood classifier.

4.2 Variation in LULC maps using Machine Learning and Maximum Likelihood Classifiers.

The classification maps produced by ML, SVM, and ANN classifiers are presented in Figure 3, 4 and 5. All classification approaches identified Bare surface as the LULC class occupying more than half of the total area, All methods identified water class as the LULC class with the smallest area. Nevertheless, some differences between the classifications of SVM, ANN and ML models were noticed. In fact, inconsistencies in classifications with all classes were observed. Table 3, 4 and 5 shows the area of each LULC class in each year with respect to the total land coverage in the study area for each classifier. The percentage share of bare surface in total area varies from 74.426 km² (66.02%) by SVM to 93.07 km² (82.56%) by ANN and 8.08 km² (81.33%) by ML in 2002. In 2012 the total area covered by built-up area varies from 33.94 km² by ML to 44.257km² by SVM covering 30.11% and 39.256% of the area for ML and SVM respectively. While in 2022, Vegetation varied from 5.88km² (5.21%) by ANN to 14.8 km² (13.127%) by SVM, Water also varied from 2.39 km² (2.12%) by ML to 3.12 km² (2.85%) by ANN. All models were strongly influenced by Poor quality in the land sat 7 ETM+ (2012) image. Overall maximum coverage of built-up land was classified by the SVM method in 2012, whereas least coverage of built-up land was classified by ML. On the other hand, the highest coverage of bare surface is found by the ANN classifier in 2002, followed by ML, while the least coverage is found by SVM. The coverage of water bodies, ANN classifier has the highest coverage in 2022, followed by SVM classifiers, while ML has the least coverage, whereas SVM has the highest coverage of vegetation followed by ANN and ML (Table 4 and 5). This indicates a variation in LULC maps generated by the three classifiers such as SVM ANN and ML probably due to the differences in their learning style. This is in agreement with the findings of Talukdar *et al.* (2020) who reported that there were variations in LULC classification generated by SVM and ANN in a study carried out in River Ganga from Rajmahal to Farakka barrage, India.

4.3 Accuracy Assessment

4.3.1 Overall Accuracy and kappa Coefficient

Confusion matrices of each classification algorithm were produced to analyze classes' separation performance. Each classifier was assessed with overall accuracy (OA) and Kappa Coefficient (KC). The results

SLU JST
Sule Lamido University Journal of Science & Technology Vol. 7 No. 1 [June, 2023], pp. 97-115
https://doi.org/10.56471/slujst.v7i.380
Online ISSN: 2736-0903
Print ISSN: 2736-089X
www.slujst.edu.ng

derived with the SVM technique have the highest overall accuracy (95.5%, 87.7% and 90%) and Kappa Coefficient (0.94, 0.83 and 0.87) for 2022, 2012 and 2002 respectively, closely followed by ANN which correctly classified the features with overall accuracies of (89.5%, 87.5% and 85%) and Kappa Coefficient (0.86, 0.85 and 0.80) for 2022, 2012 and 2002, of the cases and finally The Maximum Likelihood estimation presented a correct classification percentage of 84.5%, 70% and 82.5% and Kappa Coefficient (0.83. 0.60 and 0.767) for 2022, 2012 and 2002 respectively. The Overall Accuracy (OA) and Kappa Coefficient (KC) of the classified images are presented in Table 6.

Table 6.Overall Accuracy and Kappa Coefficient

	SVM		ANN		ML	
Year	**OA**	**KC**	**OA**	**KC**	**OA**	**KC**
2002	90%	0.87	85%	0.80	82.5%	0.767
2012	87.7%	0.83	87.5%	0.85	70%	0.60
2022	95.5%	0.94	89.5%	0.86	84.5%	0.83

The result was seriously influenced by the training samples. According to Anderson *et al.* (1976) a minimum level of accuracy approximating 85% is adequate for classification of LULC features. On the other hand, Fleiss *et al.* (2003) stipulated that, a Kappa value above 0.75 is sufficient for LULC classification. This means that the Overall accuracy of the classification result generated by SVM, that is 95.5% (2002), 87.5% (2012) and 90% (2022) were excellent. The SVM classifier also produced kappa values above 0.75, that is Kappa coefficient of 0.87 (2002), 0.83 (2012) and 0.94 (2022) signifying a substantial and almost perfect kappa coefficient, indicating an unbiased classification assessment. This result agrees with the result obtained by Leewen *et al.* (2020) who reported that that SVM achieved a minimum level of accuracy with an overall accuracy of 96.58% and Kappa value of 0.9591 and also recorded the highest as compared with RF and ANN in LULC classification of medium resolution optical satellite image focusing on inundated areas in flat area in South of Hungary. The highest accuracy achieved by SVM is attributed to the classifier's capacity to produced meaning full result with minimal training sites. This demonstrated that SVM classifier is more effective than ANN and ML classifier in LUC classification and therefore good enough for change detection analysis.

4.3.2 User and Producer Accuracy for Various LULC classes

However, the user and producer accuracies varied between the LULC classes and classifiers. SVM obtained the highest Producer Accuracy (PA) in water (100%) and the highest User Accuracy (UA) in vegetation (100%) in 2002. In contrast, the SVM obtained lower user accuracy on the bare surface (80%). In 2012, SVM obtained a low user accuracy of 80% on bare surface, while ANN achieved a lower producer accuracy of 81.3% on bare surface and a lower user accuracy of 48% on builtup. Low user and producer accuracies for built-up (UA: 50%, PA: 71.4%) and bare surfaces (UA: 80%, PA: 69.2%) were also obtained by ML. likewise, Low user and producer accuracies in built-up (UA: 48%, PA: 83%) and bare surfaces (UA: 82%, PA: 81.3%) were however achieved by ANN. in 2022, both producer and user accuracy were highest in water (100%) using SVM classifier, while low user (70%) and producer (79.5%) accuracy was obtained for bare surface by ML. The User and Producer Accuracy for Various LULC classes are presented in Table 7.

Table 7. User and Producer Accuracy for Various LULC classes

	Year	User Accuracy (UA)				Producer Accuracy (PA)			
		Built-up	**Veg.**	**Water**	**Bare surface**	**Built-up**	**Veg.**	**water**	**Bare surface**
SVM	2002	90%	100%	90%	80%	90%	83%	100%	88.9%
	2012	90%	100%	80%	80%	95%	78.4%	92.9%	82%
	2022	94%	94%	100%	94%	92.2%	95.9%	100%	94%
ANN	2002	80%	90%	90%	80%	100%	75%	93.6%	76.9%
	2012	48%	90%	90%	82%	83%	81.8%	81.8%	81.3%

SLU JST
Sule Lamido University Journal of Science & Technology Vol. 7 No. 1 [June, 2023], pp. 97-115
https://doi.org/10.56471/slujst.v7i.380
Online ISSN: 2736-0903
Print ISSN: 2736-089X
www.slujst.edu.ng

	2022	92%	82%%	100%	84%	88.5%	83.7%	98.04%	87.5%
ML	2002	70%	100%	80%	80%	100%	66.7%	100%	80%
	2012	50%	90%	60%	80%	71.4%	64.3%	83.3%	69.2%
	2022	94%	84%	90%	70%	72.3%	91.3%	100%	79.5%

The highest user and producer accuracies were achieved by SVM whereas the ML classification approach created the lowest producer's and user's accuracies for the individual classes. The higher producer accuracy obtained in the LULC classes could be due to their very low spectral confusion. The lower user accuracy could be attributed to the relatively poor quality of the 2012 image (Land sat 7 ETM+) used in the classification. All three classifications show relatively large errors for the vegetation class. The main reason for this might be the mixed pixels in the vegetation due to the resolution of land sat data. Highest user and producer accuracy in bare surface was produced by SVM among the three classifiers in 2022 probably due to the higher spectral quality of Land sat 8 OLI data used and based on the SVM relatively small number of complexes decision boundaries. The above assertion is supported by Abdi (2020) who affirmed that the ability of SVM to produce the highest accuracy for bare surface was based on a relatively small number of complex decision boundaries. On the other hand, the lowest user and producer accuracies for built up and bare surface was obtained by ANN and ML algorithm highlighting the difficulty of the two classifiers to distinguish the features. The finding supports the assertion of Leewen (2020) that urban class was poorly classified by ANN in LC classification carried out in South of Hungary.

4.4 Land use Land cover change Detection

Overall accuracy and Kappa statistics agree that the LULC maps derived with the SVM technique is the most accurate of the three sets of LULC maps derived in this work. Hence SVM LULC maps were selected for LULC change analysis. In 2002 which is the base year, Bare surface occupied the largest percentage 66.02% (74.426km²) out of the total area (112.74 Km²) followed by Vegetation which occupied 16.40% (18.486Km²) and Built-up which occupied 14.62% (16.481Km²). Water on the other hand occupied 2.97% (3.347Km²). The Land use Land cover statistics of Yola North from 2002 to 2022 are shown Table 8 and Figure 6.

Table 8. Land use Land cover statistics of Yola North from 2002 to 2022.

	2002		**2012**		**2022**	
Class name	Area (Km^2)	%	Area (Km^2)	%	Area (Km^2)	%
Built-up	16.481	14.62	44.257	39.26	58.556	51.94
Vegetation	18.486	16.40	16.581	14.71	14.80	13.13
Water	3.347	2.97	3.921	3.48	2.683	2.38
Bare surface	74.426	66.02	47.981	42.56	36.701	32.55
Total	**112.74**	**100**	**112.74**	**100**	**112.74**	**100**

Sule Lamido University Journal of Science & Technology Vol. 7 No. 1 [June, 2023], pp. 97-115
https://doi.org/10.56471/slujst.v7i.380
Online ISSN: 2736-0903
Print ISSN: 2736-089X
www.slujst.edu.ng

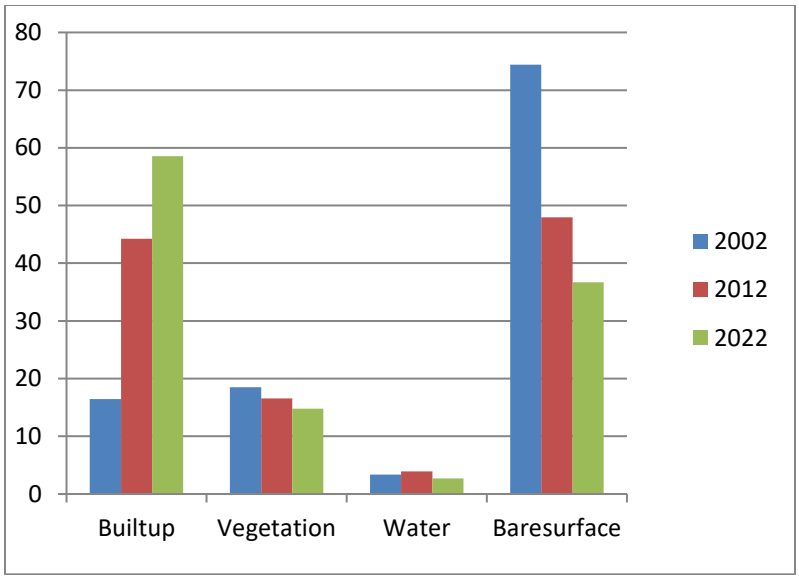

Figure 6. Land Use Land Cover Statistics of Yola North in 2002, 2012 and 2022.

The result clearly shows that the land cover classification of the study area has undergone continuous spatial changes over the past two decades based on the change detection results and land cover classification accuracy. Table 9 and Figure 7 present the changes in the land cover of Yola-North city as categorized into two different periods. The first, from 2002 to 2012 and the second, from 2012 to 2022. The major land cover types that experienced tremendous changes are built-up land, bare surface and natural vegetation. The result of the two different periods revealed substantial growth in only one land use class, which is the built-up/urban area. The built-up area grew by 27.78km² (24.64%) during the first period, 14.30km² (12.68%) during the second period, and during the whole study period from 2002 to 2022, the built-up area expanded by 42.07km² (37.32%) at an annual growth rate of 2.104 km² per annum. As the built area increases, the study result revealed a corresponding decrease in other land cover classes. It shows that vegetation lost 1.9km² between 2002 and 2012, indicating a negative change of 1.69%. Bare soil lost 26.44km² between 2002 and 2022, indicating a negative change of 23.46%, while Water bodies gain 0.57km² between 2002 and 2012, indicating a positive change of 0.51%. In contrast, Water bodies suffered a loss from the total land area between 2012 and 2022, while the result also revealed a substantial decrease in the city's vegetation and bare soil by approximately 1.78km² and 11.28km² indicating a negative change of 1.58% and 10.01% respectively. During the whole study period, that is, between 2002 and 2022 vegetation witnesses a substantial decreased of about 3.69km². Bare surface and Water also recorded a decrease in land area by 37.73km² (-33.47%) and 0.66km² (-0.59) respectively.

Table 9. Area and percentage change of LULC in Yola North during the different periods

	2002-2012		2012-2022		2002-2022		Annual change	
Class name	**Area (Km^2)**	**%**	**Area (Km^2)**	**%**	**Area (Km^2)**	**%**	**Area (Km^2)**	**%**
Built-up	27.78	24.64	14.30	12.68	42.07	37.32	2.104	1.87
Vegetation	-1.90	-1.69	-1.78	-1.58	-3.69	-3.27	-0.185	-0.009
Water	0.57	0.51	-1.24	-1.1	-0.66	-0.59	-0.033	-0.0017
Bare surface	-26.44	-23.46	-11.28	-10.01	-37.73	-33.47	-1.887	-0.059

Sule Lamido University Journal of Science & Technology Vol. 7 No. 1 [June, 2023], pp. 97-115
https://doi.org/10.56471/slujst.v7i.380
Online ISSN: 2736-0903
Print ISSN: 2736-089X
www.slujst.edu.ng

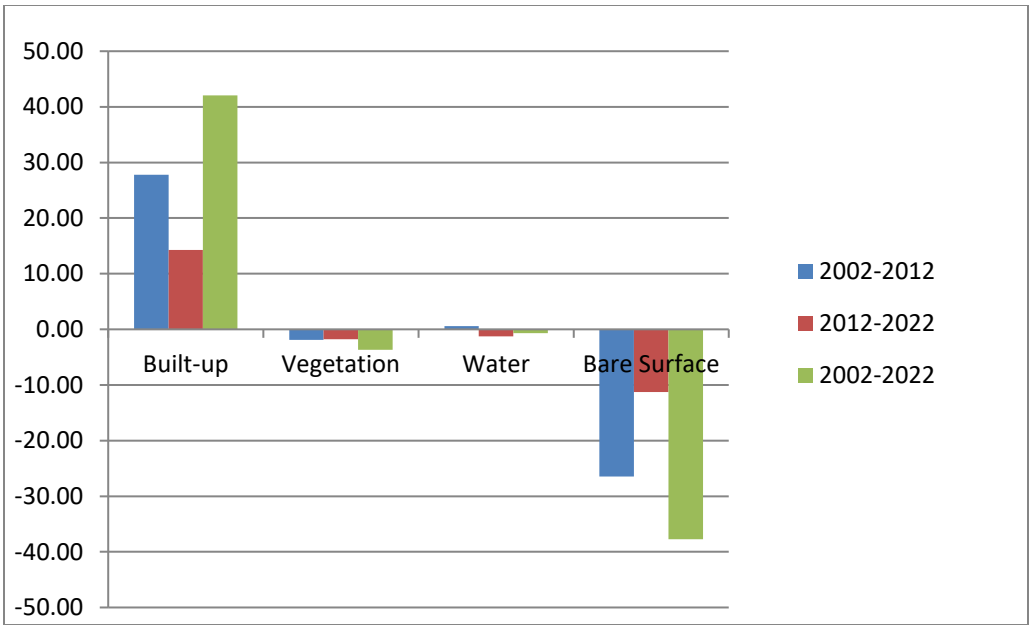

Figure 7. Net gains and losses in LULC in Yola North between 2002 and 2022

The historical land cover change result suggests both positive and negative changes observed among the different land cover classes in Yola-North, during the study period, as shown in Figure 7. From change analysis of land use land cover between 2002 and 2022 it was observed that there is a substantial increase in built-up areas and decrease in bare-land, vegetation and water. On the other hand, water slightly increased in 2012 and eventually decreased in 2022. This suggests that the study area is seriously experiencing continuous change in LULC features initiated by physical expansion of the settlements occasioned by the prevailing rapid urbanization process probably due to population expansion. The above assertion is supported by Muhammad *et al.* (2018) who affirmed that built up areas in Yola North Local Government Area is increasing while vegetation and bare surface is decreasing. The rate of urban expansion in this study however is slower than what was reported in other cities. In Lagos for instance, Faisal *et al*. (2021) reported an average annual increase of approximately 3.86% between 1990 and 2020. Dangula and Manaf (2020) reported that Sokoko city expanded at 2.3% between 1990 and 2015. Higher annual growth rate of 4.2% was also reported in Fez, Morocco (El Garouani *et al.*, 2017). This may however not be surprising as these cities are larger and perform higher socio-economic functions than Yola-North LGA.

4.4.1 Transitions between LULC features

The direction of changes as presented in Table 10 indicates that about 0.05, 37.73 and 3.69 km² of water, bare surface, and vegetation respectively were converted to built-up land During the study period. In this way, built-up area increased by approximately 37.32%. On the other hand, the land area under natural vegetation of 0.38 and 0.37 km² were respectively converted to bare surface and water bodies resulting to a decrease of 3.27% in the area of natural vegetation. The land use and land cover transition matrix are shown in figure 8 and Table 10.

Sule Lamido University Journal of Science & Technology Vol. 7 No. 1 [June, 2023], pp. 97-115
https://doi.org/10.56471/slujst.v7i.380
Online ISSN: 2736-0903
Print ISSN: 2736-089X
www.slujst.edu.ng

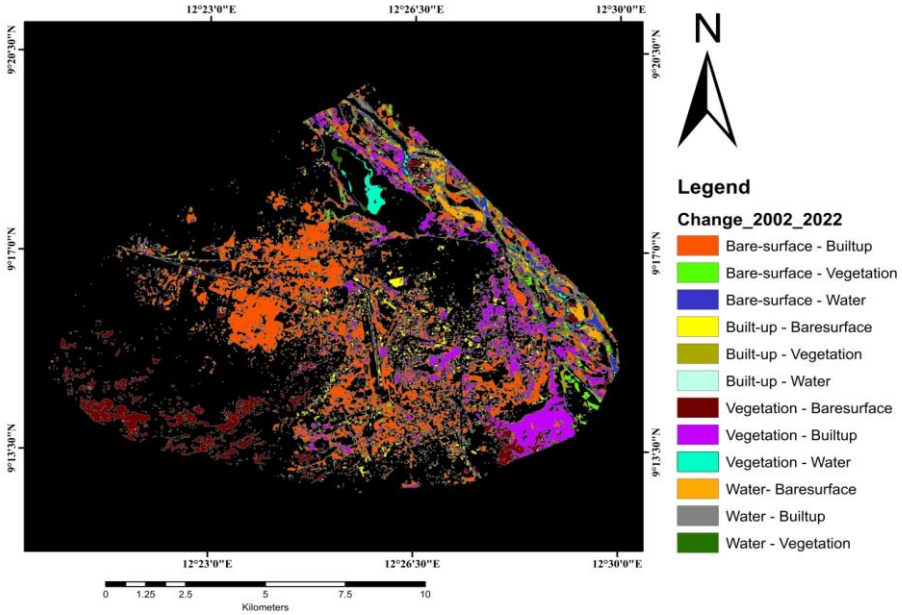

Figure 8. Transitions matrix of LULC in Yola-North between 2002 and 2022

Table 10. Transition statistics of LULC in Yola North between 2002 and 2022

Change_2002-2022	Area Change (Km²)
Water - Built-up	0.05
Water – Vegetation	0.40
Water - Bare surface	0.21
Built-up – Vegetation	0.05
Built-up – Water	0.04
Built-up - Bare surface	0.04
Bare surface - Built-up	37.73
Bare surface – Vegetation	0.30
Bare surface – Water	0.13
Vegetation - Built-up	3.69
Vegetation – Water	0.37
Vegetation - Bare surface	0.38

The study observed that, during the study period, significant portion of bare-land and vegetations got converted in to urban areas. This is in consistent with El Garouani *et al.* (2017) who assert that the general patterns and trends of land use change in Fez, Morocco revealed that, a significant portion of land area was converted from agricultural, forest and range-land use to urban use (impervious area) and also Mehrabi *et al*. (2019) noted that, bare land and vegetation were converted to built-up in Rafsanjan city of Iran. This was accounted for by some of the construction project executed by the state government, such as construction of new roads and allocation of new layout for residential purpose, which lead to the clearance of much vegetation.

4.4.2 Spatial Pattern and Trend

The spatial pattern of LULC between 2002 and 2022 in the study area conversion was radial as it occurred in all direction, however it is more pronounced to the western and south eastern part of the study area where development land was supposedly more accessible. The Vegetation and bare surface were most vulnerable LULC

Sule Lamido University Journal of Science & Technology Vol. 7 No. 1 [June, 2023], pp. 97-115
https://doi.org/10.56471/slujst.v7i.380
Online ISSN: 2736-0903
Print ISSN: 2736-089X
www.slujst.edu.ng

classes as the area expanded. The pattern and the trend of land use and land cover conversion is shown by cubic trend analysis (figure 9)

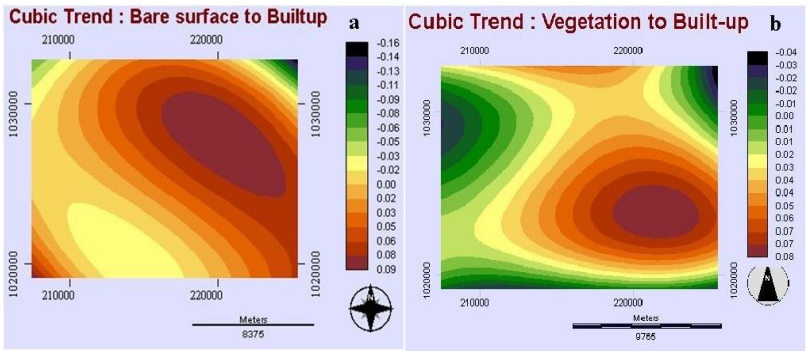

Figure 9. Pattern and trend of land conversion between 2002 and 2022 from (a) Bare surface to Built-up and (b) Vegetation to Built-up.

While the conversion of bare surface inclined to the southwestern and eastern part of the city, conversion of vegetation was more to the southeast. Bare surface and vegetation were severely converted to built-up area during the study period which indicates a forward trend in Built-up and a backward trend in vegetation and bare surface. This followed the natural urban development process where cities expand along ring roads from city center to the fringe, as obtained in Sokoto city of Sokoto state, Nigeria (Dangula and Manaf, 2020).

5. Conclusion

This study demonstrates that SVM is well suited for LC classification in Yola North. SVM and ANN successfully classified LC on Landsat-8 images of 2022 and Land sat 7 images of 2002. However, LC classification using SVM was slightly more accurate than that obtained by employing the ANN and ML for LULC changes in Yola-North. Consequently, it can be concluded that the SVM was computationally efficient and had a high recognition rate. The classification accuracy obtained by ML was relatively the lowest in this study because of the complex landscape and insufficient training sample. The ANN was better only when classifying built-up and water in 2002 and 2022. SVM better appraised land classes with small numbers of pixels. That is, in all the three years (2002, 2012 and 2022) SVM identified water, although the water regions were very small. All models accurately distinguished products of vegetation and water from other LC. Spatial resolution substantially affects LC accuracy especially for land sat 7 (2012). The study demonstrates that built-up area, vegetation, water and bare surface in Yola North can be discriminated using the SVM land cover classification technique. Furthermore, findings from the land use change over the last two decades (2002–2022) in Yola North LGA showed the results to be feared. The land use change scenarios modeled in LULC indicate an increase in built-up and a decrease in vegetation areas, bare surface and water resources, both of which can be considered a warning of agricultural land loss and without proper planning it could cause a severe consequence for the environment, society, and overall sustainability. By prioritizing sustainable development, integrating smart growth principles, and fostering collaboration among stakeholders, it is possible to mitigate these negative effects and create more resilient, livable, and equitable urban environments. The spatially and temporally consistent mapping of LULC can provide a better understanding of landscape dynamics, which is essential for biodiversity conservation and LULC change monitoring. The combined use of the Land Change Modeler (LCM) and Cubic trend analysis for modeling LULC change is likely to make the closest predictions to reality using the transition probability matrix. It is therefore recommended that feature urban development schemes should adopt a sub-urban type of development to reduce the pressure on infrastructure in the central district. Geospatial techniques should be adopted by Government and NGOs to help in understanding of land use planning, provision of essential information for monitoring, evaluation, land management, environmental impact assessment, infrastructure planning, resource management, and policy development. It helps ensure that land use decisions are implemented effectively, resources are managed sustainably, and environmental impacts are

Online ISSN: 2736-0903
Print ISSN: 2736-089X
www.slujst.edu.ng

minimized. It is also suggested that future studies of this nature could be carried out in other major Nigerian cities for the purpose of drawing inference.

References

Abdi, A.M. (2020). Land cover and land use classification performance of machine learning algorithms in a boreal landscape using Sentinel-2 data. *GIScience & Remote Sensing*, 57(1), 1-20. DOI: 10.1080/15481603.2019.1650447

Abera, W., Tamene, L., Kassawmar, T., Mulatu, K., Kassa, H., Verchot, L., & Quintero, M. (2021). Impacts of land use and land cover dynamics on ecosystem services in the Yayo coffee forest biosphere reserve, southwestern Ethiopia, *Ecosystem Services*, 50, 101338. https://doi.org/10.1016/j.ecoser.2021.101338.

Adeyemi, A.A., & Oyeleye, H.A. (2021). Evaluation of land-use and land-cover changes cum forest degradation in Shasha forest reserve, Osun state, Nigeria using remote sensing. *Tanzania Journal of Forestry and Nature Conservation*, 90(2), 27-40. Retrieved from https://www.ajol.info/index.php/tjfnc/article/view/210925

Adhikary, P.P., Barman, D., & Madhu, M. (2019). Land use and land cover dynamics with special emphasis on shifting cultivation in Eastern Ghats Highlands of India using remote sensing data and GIS. Environmental Monitoring and Assessment 191, 315. https://doi.org/10.1007/s10661-019-7447-7

Aljenaid, S.S., Ghadeer, R. Kadhem G.R., Manaf F. AlKhuzaei, M.F., Jobair B., & Alam, J.B. (2021). Detecting and Assessing the Spatio-Temporal Land Use Land Cover Changes of Bahrain Island during 1986–2020 Using Remote Sensing and GIS. *Earth Systems and Environment*. https://doi.org/10.1007/s41748-022-00315-zJensen

Anad, A. (2017). Accuracy Assessment. Retrieved from https://www.researchgate.net/publication/324943246

Anderson, J.R., Hardy, E.E., Roach, J.T., & Witmer, R.E. (1976). A land use and land cover classification system for use with remote sensor data. *United State Geological Survey Professional Paper*, No. 964. USGS, Washington, D.C. Retrieved from https:// pubs.usgs.gov/ pp/ 0964/ report.Pdf

Ayele, G.T., Tebeje, A.K., Demissie, S.S., Belete, M.A., Jemberrie, M.A., Teshome, W.M.,….Teshale, E.Z. (2018).Time Series Land Cover Mapping and Change Detection Analysis Using Geographic Information System and Remote Sensing, Northern Ethiopia. *Air, Soil and Water Research*, 11, 1–18. DOI: 10.1177/1178622117751603

Birzhandi, P., Kim, K., & Youn, H. (2022). Reduction of training data for support vector machine: a survey. *Soft Computing*, 26, 1-14. Doi: 10.1007/s00500-022-

Congalton, R.G., & Green, K. (2019). Assessing the Accuracy of Remotely Sensed Data: Principles and Practices, Third Edition (3rd ed.). *CRC Press*. https://doi.org/10.1201/9780429052729

Dangula, M., & Manaf, L. A. (2020). Spatio-temporal analysis of land use/land cover dynamics in Sokoto Metropolis using multi-temporal satellite data and Land Change Modeler. *Indonesian journal of geography*. DOI:10.22146/ijg.46615. Retrieved from https://www.researchgate.net/publication/348514057

Das, J. (2021, August 21). Radiometric and Atmospheric Correction of Satellite image in Arcgis [Video file]. Video posted to https://www.youtube.com/watch?v=fAxONnFEb98

Delalay, M., Tiwari, V., Ziegler, A.D., Gopal, V., & Passy, P. (2019). Land-use and land-cover classification using Sentinel-2 data and machine-learning algorithms, operational method and its implementation for a mountainous area of Nepal. *Journal of Applied Remote Sensing*, 13(1), 247–259. doi:10.1117/1.JRS.13.014530.

El Garouani, A., Mulla, D.J., El Garaouani, S., & Knight, J. (2017). Analysis of Urban growth and sprawl from Remote sensing data: Case of Fez, Morocco. *International Journal of sustainable Built Enviroment*, 6(1), 160-169. https://doi.org/10.1016/j.ijsbe.2017.02.003

Ettehadi, O., Paria, S. K., Elif S., & Ugur, A. (2019). Separating Built-Up Areas from Bare Land in Mediterranean Cities Using Sentinel-2A Imagery. *Remote Sensing*, 3(345), 11. https://doi.org/10.3390/rs11030345

Faisal, A. K., Yue, W., Abdullahi, G. A., Hamed, R., & Akram, A. N. A. (2021). Analyzing urban growth and land cover change scenario in Lagos, Nigeria using multi-temporal remote sensing data and GIS to mitigate flooding. *Geomatics, Natural Hazards and Risk*, 12(1), 631-652. DOI: 10.1080/19475705.2021.1887940

Online ISSN: 2736-0903
Print ISSN: 2736-089X
www.slujst.edu.ng

Fleiss, J.L, Levin, B., & Paik, M.C. (2003). The measurement of interrater agreement. In: Shewart WA, Wilks SS, editors. Statistical methods for rates and proportions. Hoboken, NJ: John Wiley and Sons Inc, 598–626. Retrieved from https://onlinelibrary.wiley.com/doi/10.1002/0471445428.ch18

Green L, Fry AF, Myerson J (1994) Discounting of delayed rewards: a life-span comparison. Psychol Sci 5(1):33–36. https:// doi. org/10. 1111/j. 1467- 9280. 1994. tb006 10.x

Hamad, R. (2020). An assessment of artificial neural networks, support vector machines and decision trees for land cover classification using sentinel-2A data. *Applied Ecology and Environmental Sciences*, 8(6), 459–464. Doi: 10.12691/aees-8-6-18

International Business Machine cloud education (2020). Definition of machine learning. Retrieved from https://www.ibm.com/cloud/learn/machine-l

Jensen, J. R. (2005). Introductory digital image processing: A Remote sensing perspective, 3rd edition. *Scientific Research*. Retrieved from https://www.scirp.org/(S(351jmbntvnsjt1aadkposzje))/reference/ReferencesPapers.aspx?ReferenceID=2001065

Jimeta Population. (2015). Retrieved September 2, 2022, from http://population.city/nigeria/jimeta/

Kadavi, P.R. & Lee, C.W. (2018). Land cover classification analysis of volcanic island in Aleutian arc using an artificial neural network (ANN) and a support vector machine (SVM) from landsat imagery. *Geosci*, 22, 653–665. Retrieved from https://link.springer.com/article/10.1007/s12303-018-0023-2

Leeuwen, B. V., Tobak, Z., & Kovacs, F. (2020). Machine learning techniques for land use/land cover classification of medium resolution optical satellite imagery focusing on temporary inundated areas. *Journal of Environmental Geography*, 13(12), 43–52. DOI: 10.2478/jengeo-2020-0005 ISSN 2060-467X

Mehrabi, A., Khabazi, M., Almodaresi, S.A., Nohesara, M., Derakhshani, R., Derakhshani, R. (2019). Land Use Changes Monitoring over 30 Years and Prediction of Future Changes Using Multi-Temporal Landsat Imagery and the Land Change Modeler Tools in Rafsanjan City (Iran). *Sustainable Development of Mountain Territories*, 11(39). Retrieved from https://ssrn.com/abstract=3405670

Moumni, A., & Lahrouni, A. (2021). Machine Learning-Based Classification for Crop-Type Mapping Using the Fusion of High-Resolution Satellite Imagery in a Semiarid Area. *Hindawi Scientifica*, 8810279, 20. https://doi.org/10.1155/2021/8810279

Muhammad, B. U., Ismaila, A.B., & Aliyu. I. (2018). An Analysis of Urban Growth Pattern in Yola-North Local Government Area, Adamawa State, Nigeria. *Savanna: Journal of Environmental and Social Sciences*, 24(3). Retrieved from https://www.academia.edu/38701947

Nedd, R., Light, K., Owens, M., James, N., Johnson, E., & Anandhi, A. (2021). A Synthesis of Land Use/Land Cover Studies: Definitions, Classification Systems, Meta-Studies, Challenges and Knowledge Gaps on a Global Landscape. *Land*, 10(9), 994. https://doi.org/10.3390/land10090994

Nogueira, K., Otávio, A.B., Jefersson P.A. & Santos, D. (2017). Towards better exploiting Convolution neural networks for remote sensing scene classification. *Pattern Recognition*, 61,539-556, https://doi.org/10.1016/j.patcog.2016.07.001.

Petitjean, F., Inglada, J., & Gancarski, P. (2012). Satellite Image Time Series Analysis Under Time Warping, *IEEE Transactions on Geosciences and Remote Sensing*, 50(8), 3081-3095. Doi: 10.1109/TGRS.2011.2179050.

Rendy, k. (2021*). Google Earth Engine Machine Learning for Land Cover Classification with Code*. Retrieved September 2, 2022, Retrieved from https://www.analyticsvidhya.com/blog/2021/04/google-earth-engine-machine-learning-for-land-cover-classification-with-code/

Shih, H., Stow, D. A., & Tsai, Y. H. (2019). Guidance on and comparison of machine learning classifiers for Landsat-based land cover and land use mapping. *International Journal of Remote Sensing*, *40*(4), 1248-1274. https://doi.org/10.1080/01431161.2018.1524179

Soni, S. K. (2011), Crop Area Estimation for Bundi Tahsil of Rajasthan using Remote Sensing and GIS Technique, *Geospatial World Forum, Hyderabad, India,* 18(21). Retrieved from http://wgbis.ces.iisc.ernet.in/energy/paper/MODIS/intro.htm#gmlc

Sophia, R., & Julius, N., (2017). Accuracy Assessment of Land Use Land Cover Classification Using Remote Sensing and GIS. *International Journal of Geosciences*. 8, 611-622. DOI:10.4236/ijg.2017.84033

Online ISSN: 2736-0903
Print ISSN: 2736-089X
www.slujst.edu.ng

Talukdar, S., Singha, P., Mahato, S., Fahad, S., Pal, S., Liou, Y.A., & Rahman, A. (2020). Land Use Land Cover Classification by Machine Learning Classifiers for Satellite Observations: A Review. *Remote Sensing*, 12(7), 1135 https://doi.org/10.3390/rs12071135

Traoré, F., Bonkoungou, J., Compaoré, J., Kouadio, L., Wellens, J., Hallot, E., & Tychon, B. (2019). Using Multi- Temporal Landsat Images and Support Vector Machine to Assess the Changes in Agricultural Irrigated Areas in the Mogtedo Region, Burkina Faso. *Remote Sensing*; 11(12):1442. DOI: https://doi.org/10.3390/rs11121442

United State Geological Survey. (2022*). What are the band designations for the Landsat satellites?* Retrieved from https://www.usgs.gov/faqs/what-are-band-designations-landsat-satellites

Valero, M.J.A., & Alzate, A. B.E. (2019). Comparison of maximum likelihood, support vector machines, and random forest techniques in satellite images classification. *Tecnura*,23(59),13-26. https://doi.org/10.14483/22487638.14826

Weather Spark. (2021). *Jimeta Climate, Weather By Month, Average Temperature (Nigeria)*. Retrieved from https://weatherspark.com/y/71692/Average-Weather-in-Jimeta-Nigeria-Year-Round#Sections-Temperature

Yan, J., Wang, L., Song, W., Chen, Y., Chen, X., & Deng, Z. (2019). A time-series classification approach based on change detection for rapid land cover mapping. *Journal of Photogrammetry and Remote Sensing*, 158, 249-262. https://doi.org/10.1016/j.isprsjprs.2019.10.003.

Yu, Z., Di, L., Yang, R., Tang, J., Lin, L., Zhang, C., Rahman, M.… & Sun, Z. (2019, July). *Selection of Landsat 8 OLI Band Combinations for Land Use and Land Cover Classification. Paper presented at 8th International Conference on Agro-Geo-informatics, Istanbul, Turkey.* doi:10.1109/Agro-Geoinformatics.2019.8820595

